

## Impact of climate change on flood and drought events in Huaihe River Basin, China

Chuanguo Yang, Zhongbo Yu, Zhenchun Hao, Jiangyun Zhang and Jianting Zhu

### ABSTRACT

The impact of climate change on floods and droughts in Huaihe River Basin is studied using a coupled land-surface hydrology model and continuous wavelet transform technique. Observed temperature in the basin has increased by approximately 0.228 °C per decade since 1951. Observed precipitation and simulated and observed streamflows are used to grade flood and drought events. Two composite grading indices derived from the three series using different weight values are defined for reducing uncertainties caused by errors of observation and simulation and the effect of human activity on observed streamflow. The frequency of flood and drought events is quantified using the Morlet wavelet transform and compared with the trend of average temperature to test for any relationship between climate change and flood/drought frequency. This study shows that flood and drought events have occurred more frequently since the 1980s. The trend of flood and drought events is positively related to climate warming with a coefficient of determination of 0.88 in the Huaihe River Basin.

**Key words** | climate change, drought, flood, Huaihe River Basin, hydrologic simulation

**Chuanguo Yang**  
**Zhongbo Yu** (corresponding author)  
**Zhenchun Hao**  
State Key Laboratory of Hydrology-Water Resources and Hydraulic Engineering, Hohai University, #1 Xikang Road, Nanjing 210098, China  
E-mail: [zyu@hhu.edu.cn](mailto:zyu@hhu.edu.cn)

**Zhongbo Yu**  
Department of Geoscience, University of Nevada Las Vegas, Las Vegas, NV 89154-4010, USA

**Jianguo Zhang**  
Hydrology and Water Resources Department, Nanjing Hydraulic Research Institute, Nanjing 210032, China

**Jianting Zhu**  
Division of Hydrologic Sciences, Desert Research Institute, Las Vegas, NV 89119, USA

### INTRODUCTION

Serious natural disasters affecting agriculture, industry and human life, such as floods and droughts, have been the focus of attention in recent decades (Waters *et al.* 2003; Jiang *et al.* 2005; Lehner *et al.* 2006; IPCC 2007; Bates *et al.* 2008). Climate warming and increased climate variability (e.g. increased precipitation intensity and variability) have been projected by many global circulation models (GCMs) for the next 100 years by the first assessment report of the Intergovernmental Panel on Climate Change (IPCC) (Houghton *et al.* 1990). This situation may lead to more flood and drought events in many river basins of the globe, particularly at middle and high latitudes (Wetherald & Manabe 2002; Meehl *et al.* 2005; IPCC 2007; Veijalainen & Vehviläinen 2008).

Many regions have an increased risk of floods and droughts. For example, annual extreme daily flows from 195 rivers, principally in North America and Europe, were

examined in the Global Runoff Data Center (GRDC) report by Kundzewicz (2004). Although no consistent trends were found for all the rivers, the high flow in the 1990s was four times larger than in the 1960s in Europe. From a pooled study on large river basins worldwide (Milly *et al.* 2002), the observed trend of flood events has been positive since 1993 and intermittently positive since 1972. More than half of observed flow series of rivers in Scotland have recorded their highest flows since 1989 (Werrity *et al.* 2002). There has also been a global trend of drought since the 1970s, partly due to increasing temperatures (Sheffield & Wood 2008). More intense and frequent droughts have been observed due to temperature rise and increased evaporation (Burke *et al.* 2006).

Aside from climate change, human activities have also increased the risks of floods and droughts. For example,

deforested regions usually have higher flows; and water withdrawal remarkably decreases river flow in dry years in developed basins. Hence, modelling the hydrologic processes is an alternative approach in understanding the uncertainty of observed streamflows (Chun *et al.* 2009) and in representing natural responses to climate change.

This study aims to evaluate the impact of climate change on flood and drought events and to understand possible relationships between the frequency of the events and climate change in the Huaihe River Basin, China. First, the study basin and data are described. A coupled hydrologic model, a grading method of flood/drought and a wavelet transform tool are then described. The simulated and observed streamflows, grading of floods and droughts and analysis of wavelet power spectrum are then presented, and the relationship between the frequency of flood and droughts and climate change are discussed. Finally, the conclusions for this study are summarized.

## STUDY BASIN AND DATA

Huaihe River Basin is located in a semi-humid monsoon climate region of eastern China between 30°55' and 36°30' N

and 111°55' and 122°05' E (Figure 1). It covers the area from the Tongbai-Funiu Mountains in the west to the Yellow Sea in the east. As a highly developed region in terms of agriculture, the basin has a population of approximately 165 million over a total area of 270,000 km<sup>2</sup> (i.e. population density of 611 people per square kilometre). The basin is drained by Huaihe River (1,078 km), Yishusi River and south part of the Great Canal.

The topography of the basin is characterized by low plains with numerous lakes and depressions, except in the middle high mountains near the basin boundaries. Rainfall mainly occurs in the summer from June to September, with large annual and seasonal variability. During the last several decades, floods and droughts have caused serious damage to local industry, agriculture and human life.

More than 30 meteorological stations have provided daily rainfall and temperature data for the basin from 1951 to 2006. These meteorological stations adequately cover the entire basin with spatially distributed data (Figure 1). Radiation, wind velocity, pressure and other meteorological variables are used in the simulation as forcing data. Their intra-diurnal variability from 1951 to 2006 is described by the 6 h reanalysis data of the National Center for Environmental Prediction/National Center

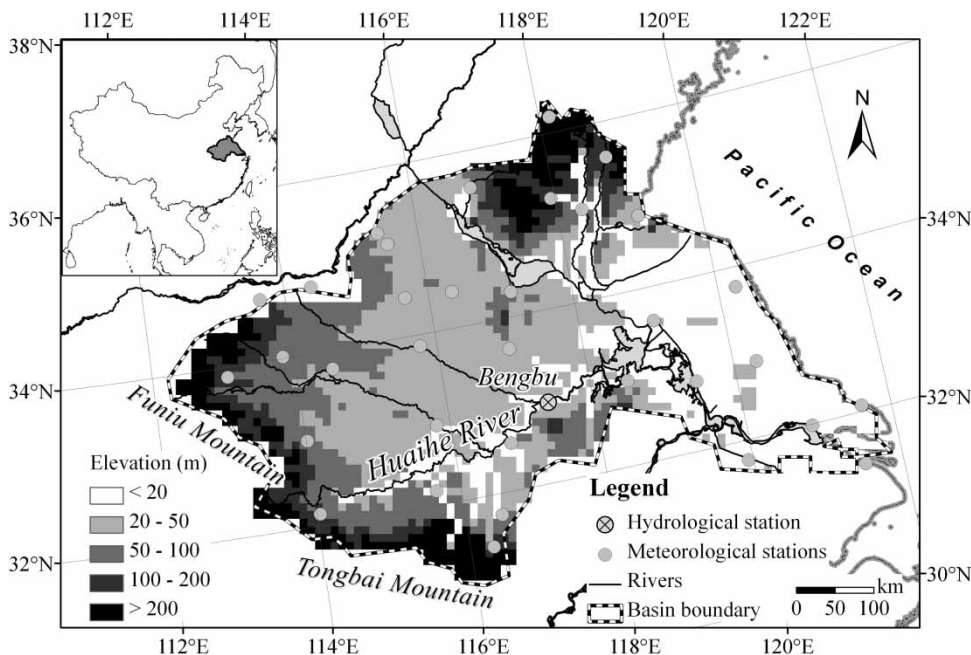


Figure 1 | Location of hydrologic station and rain gauges and topography in the Huaihe River Basin.

for Atmospheric Research (NCEP/NCAR) (Kalney et al. 1996).

Bengbu Hydrologic Station, with a drainage area of 121,000 km<sup>2</sup>, is located on the main channel near the downstream of Huaihe River (Figure 1). Calculation of the total water flux is made difficult by the complex irrigation canal network when the river flows pass the station into the low plains near Yellow Sea and Hongze Lake. Bengbu Station records long-term continuous streamflow for local indication of flood and drought events.

## MODEL AND METHODS

### Model description

In recent decades, water demand has increased as industrial and urban development has intensified. The observed streamflow cannot clearly indicate natural flow due to a large volume of water withdrawn from the river, especially during dry years. A coupled land-surface hydrologic model system (LSX-HMS) (Yu et al. 2006) has been used to simulate the long-term variability of streamflow at Bengbu Station to project natural hydrography since 1951. The forcing data consist of the NCEP/NCAR reanalysis meteorological variables and the station rainfall data.

With a scale-transferring algorithm based on predicted soil moisture and the surface water table, three major components from a distributed hydrologic model (HMS) (Yu et al. 1999; Yu 2000) at a fine-grid scale, including terrestrial hydrology, groundwater hydrology and channel-groundwater interaction, were coupled with a coarse-grid land-surface model (LSX) (Pollard & Thompson 1995) in the LSX-HMS model system. Fluxes of water, heat and moment between six soil layers, two snow layers and two vegetation layers are described in the land-surface model (LSX). Water flow in both the surface channel/lake and aquifers are predicted in the hydrologic model (HMS). Surface water flow in rivers and lakes is resolved as two-dimensional diffusion waves with eight probable orientations. The flow velocity is calculated using the Manning equation. Groundwater in an assumed one-layer aquifer is described by the two-

dimensional Boussinesq equation, with Darcy's law representing groundwater flow in the aquifers. Water fluxes between surface water and groundwater are calculated using Darcy's law according to the predicted elevation of surface water and the groundwater table. In this study, the LSX runs on the global T62 grids (c. 1.9°), similar to the resolution of NCEP/NCAR reanalysis data. The HMS runs on 10 × 10 km grids with Lambert Azimuthal projection centred at 100° E and 45° N.

Soil texture and vegetation type at coarse grids are interpolated with the global dataset of GENESIS (Global Environmental and Ecological Simulation of Interactive Systems) GCM (Pollard & Thompson 1995). Hydrogeological parameters (aquifer thickness, hydraulic conductivity and porosity) at each hydrologic grid for the assumed one-layer aquifer are derived from the look-up table of a national 1:4,000,000 geologic survey atlas.

### Grades of flood and drought events

A grading function  $G(t)$  is used to characterize droughts, normal years, and floods for the study period can be written as follows:

$$G(t) = \begin{cases} -2 & \text{for heavy drought years,} \\ -1 & \text{for drought years,} \\ 0 & \text{for normal years,} \\ 1 & \text{for flood years,} \\ 2 & \text{for heavy flood years.} \end{cases} \quad (1)$$

This grading method was suggested by the Meteorological Institute of the Chinese Meteorological Bureau (MICMB) (1981) and has been used in recent studies (e.g. Zhou et al. 2002; Jiang et al. 2005; Zhang et al. 2007). Average precipitation from May to September for each year is used to calculate the grade of flood/drought, as shown in Table 1. As a direct factor of flood and drought for a basin, the average observed and simulated streamflows at Bengbu Station from May to September are used to evaluate hydrological disasters with the grading method.

### Wavelet transform

The continuous wavelet transform (CWT) is an efficient way of detecting and analysing transient signals. Compared

**Table 1** | Flood and drought criteria for precipitation (MICMB 1981) and streamflow in Huaihe River Basin ( $S_i$  is the streamflow or average precipitation from May to September for each year;  $\bar{S}$  is the multi-annual average value of  $S_i$ ;  $\sigma$  is the standard deviation)

| Grade | Type          | Criteria   |
|-------|---------------|--|
| -2    | Heavy drought | $S_i \leq (\bar{S} - 1.17\sigma)$                          |
| -1    | Drought       | $(\bar{S} - 1.17\sigma) < S_i \leq (\bar{S} - 0.33\sigma)$ |
| 0     | Normal        | $(\bar{S} - 0.33\sigma) < S_i \leq (\bar{S} + 0.33\sigma)$ |
| 1     | Flood         | $(\bar{S} + 0.33\sigma) < S_i \leq (\bar{S} + 1.17\sigma)$ |
| 2     | Heavy flood   | $S_i > (\bar{S} + 1.17\sigma)$                             |

to the classic Fourier transform, CWT is advantageous because the time series does not need to be stationary (Torrence & Compo 1998; Nakken 1999). Providing a good balance between time and frequency localization, the Morlet wavelet is used to characterize the frequency, intensity, position of wavelet spectra peaks and duration of variations of the streamflow series. The Morlet wavelet is formulated as follows:

$$\Psi_\omega(\eta) = c_\omega \pi^{-1/4} e^{-\eta^2/2} (e^{i\omega\eta} - e^{-\omega^2/2}) \quad (2)$$

where the normalization constant  $c_\omega$  is

$$c_\omega = (1 + e^{-\omega^2} - 2e^{-3\omega^2/4})^{-1/2} \quad (3)$$

and where the non-dimensional frequency  $\omega$  is set to 6 to satisfy the admissibility condition (Torrence & Compo 1998). In this case,  $e^{-\omega^2/2}$  becomes very small and can be neglected, and  $c_\omega$  is approximately equal to 1.0. Therefore, Equation (2) can be rewritten as

$$\Psi_\omega(\eta) = \pi^{-1/4} e^{-\eta^2/2} e^{i\omega\eta} \quad (4)$$

The wavelet is not always completely localized in time. In order that edge effects can be neglected, a cone of influence is introduced. In many studies, the cone of influence is suggested to be the area where the wavelet power caused by the discontinuity drops to  $e^{-2}$  of the value at the edge (e.g. Torrence & Compo 1998; Grinsted *et al.* 2004). The statistical significance and confidence of the wavelet power are addressed in the analysis.

## RESULTS AND DISCUSSION

### Long-term continuous hydrologic simulation

From the forced observed rainfall and 6 h NCEP/NCAR reanalysis data, a long-term continuous hydrologic simulation from 1951 to 2006 was conducted with the coupled LSX-HMS model. The calibration and validation processes of the model were described by Yang *et al.* (2010). In the entire period of simulation, the distribution of vegetation type was kept unchanged. The International Satellite Land Surface Climatology Project (ISLSCP) Initiative II historical dataset (Hall *et al.* 2005) recorded that vegetation covers were changed only for one  $1 \times 1^\circ$  grid from the year 1970 to 1990 in the Huaihe River Basin.

The simulated monthly streamflows are compared with the observed streamflows at Bengbu Station in Figure 2, together with the mean monthly observed rainfall from the rain gauges upstream of Bengbu Station. The inter-annual and seasonal variations of the simulated streamflows are consistent with the observations. Both the volume and time of peaks are recorded for typical flood years (e.g. 1954, 1963, 1982, 1991 and 2003). Simulated streamflows are also consistent with the observed values in some drought years (e.g. 1953, 1966, 1978 and 1981). However, the observed streamflows are overestimated compared to the simulated results for dry years in the last decade, partly due to human-induced withdrawals which were not taken into account in the simulations (Yang *et al.* 2010). The effects of human-induced water withdrawals are evident from the remarkable decreasing trend of observed streamflows. No observed streamflow in the river channel in wet seasons of some heavy dry years (e.g. June and July in 2001) is recorded. Simulated streamflow represents the real response to natural rainfall process, especially during the dry seasons.

### Flood and drought distribution

Flood and drought events were graded using the precipitation and the simulated and observed streamflow series from May to September for each year, as shown in Figure 3. Multi-annual average monthly rainfall is 124.24 mm upstream of Bengbu Station with a large standard deviation of 31.97 mm. No remarkable trend for the precipitation

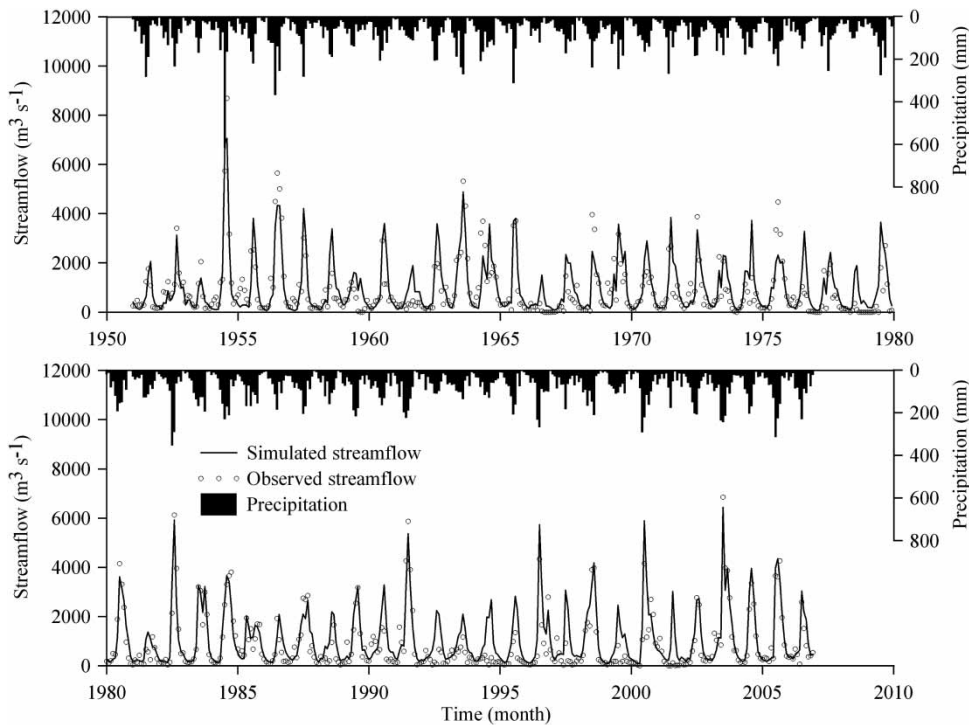


**Figure 2** | Monthly streamflows at Bengbu Station and average precipitation upstream of Bengbu Station from 1951 to 2006.

series with an increase of  $+3.6$  mm per decade is evident. Before and after 1980, three heavy floods/four floods and six heavy floods/three floods were identified, respectively, based on the observed precipitation data as shown in Figure 3(a). Meanwhile, three heavy droughts/six droughts and two heavy droughts/seven droughts were observed for the two periods.

Streamflow is the systemic response of river basin to precipitation. Before 1980, four floods ranging from  $1,606.04 \text{ m}^3 \text{ s}^{-1}$  to  $2,032.69 \text{ m}^3 \text{ s}^{-1}$  and three heavy floods were observed based on the grading with the simulated streamflow, as shown in Figure 3(b). From 1980 to 2006, six floods and four heavy floods were identified. A heavy flood event in the basin in 2007, which is second only to the flood in 1954 (Qian 2008), was reported. More floods and heavy floods have occurred in the last two decades.

Due to the influence of human activities, the observed streamflow series has a larger standard deviation of  $973.28 \text{ m}^3 \text{ s}^{-1}$  compared with the simulated streamflow with a standard deviation of  $646.45 \text{ m}^3 \text{ s}^{-1}$ . The average observed streamflow of  $1,442.65 \text{ m}^3 \text{ s}^{-1}$  decreased 20.7%

compared with the average value from the simulated streamflow. According to the grading based on the observed streamflow, eight floods and heavy floods ( $>1,763.83 \text{ m}^3 \text{ s}^{-1}$ ) and ten droughts and heavy droughts ( $<1,121.47 \text{ m}^3 \text{ s}^{-1}$ ) occurred before 1980, as shown in Figure 3(c). More flood and drought events were identified after 1980, with 11 floods and heavy floods and 12 droughts and heavy droughts.

### Composite index of flood and drought

Due to the rainfall observation error, model bias and the impact of human activity on observed streamflow, different grades were derived from different series. For example, the year of 2000 was graded to heavy flood ( $G(t) = 2$ ) based on the observed rainfall and the simulated streamflow, whereas the observed streamflow would grade it as a normal year ( $G(t) = 0$ ). A composite index of flood and drought (IFD) is therefore defined as a weighted mean of the grades derived from the three series as follows:

$$\text{IFD}(t) = w_{\text{pr}}G_{\text{pr}}(t) + w_{\text{ss}}G_{\text{ss}}(t) + w_{\text{so}}G_{\text{so}}(t) \quad (5)$$

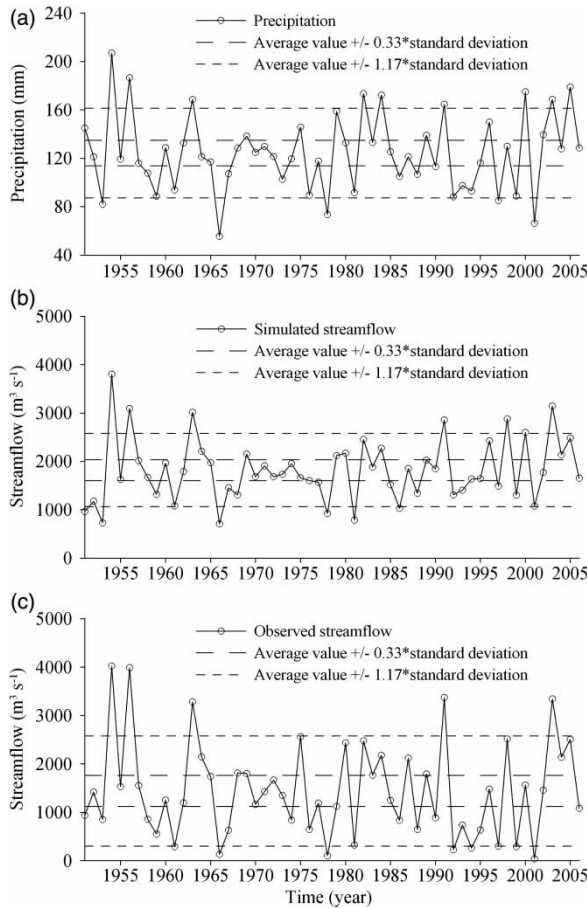


**Figure 3** | Grading floods and droughts with the MICMB method according to (a) precipitation, (b) simulated streamflow, and (c) observed streamflow.

$$\begin{cases} w_{pr} = 0.3, \\ w_{ss} = 0.7 \times a, \quad w_{so} = 0.7 \times b, \quad a + b = 1.0 \end{cases} \quad (6)$$

where  $G_{pr}(t)$ ,  $G_{ss}(t)$  and  $G_{so}(t)$  are the grades of flood/drought for the year  $t$  determined from the observed rainfall, simulated streamflow and observed streamflow series, respectively, with the MICMB grading method. Floods and droughts are addressed in hydrologic aspects. Thus, the weight of observed precipitation  $w_{pr}$  is 0.3 in Equation (5) and streamflow series has a total weight of 0.7 (i.e.  $a$  plus  $b$  equals 1.0) in Equation (6). Fewer rain gauges had continuous rainfall data before the year of 1960;  $a$  and  $b$  are therefore set to 0.1 and 0.9, respectively, to reflect the low reliability of the simulated streamflow based on the gauged rainfall data between 1951 and 1960. We used  $a = 0.4$  and  $b = 0.6$  for the well-gauged period of 1961–1990,

when human activities have a lower direct impact on streamflow. Finally,  $a = 0.7$ ,  $b = 0.3$  for dry years and  $a = 0.3$ ,  $b = 0.7$  for wet years from 1991 to 2006 as observed data have a low estimation of streamflow due to human activities (Yang et al. 2010).

Composite index  $IFDA(t)$ , defined as the absolute value of  $IFD(t)$ , is used to evaluate local water disasters such as floods and droughts:

$$IFDA(t) = |IFD(t)| \quad (7)$$

The two composite indices of flood and drought,  $IFD(t)$  and  $IFDA(t)$ , are shown in Figure 4.

The reported heavy flood of 2007, which is second to the flood of 1954, has a value of 2.0 for both  $IFD$  and  $IFDA$ . The index  $IFD$  reveals that scattered flood and drought events were distributed over the period of 1950s, 1960s and 1970s, whereas floods and droughts were almost consistent during alternate years since 1980s, becoming more severe in the last two decades. We calculated the averaged values of  $IFDA$  to represent the extent of water hazards of both flood and drought for the six decades from 1951 to 2007. The 1970s observed normal levels of flood and drought, while the 1990s and 2000s were the most severe decades in terms of water hazards.

### Period analysis of floods and droughts

The continuous Morlet wavelet transform was used to detect the occurrences of flood and drought events based on the observed and simulated streamflow series in Huaihe River Basin. The wavelet power spectrum of floods and droughts derived from the observed streamflow series ranged from 2 to 19 years, as shown in Figure 5. The 8-year period was influenced by edge effects. The shaded regions highlighting >90% confidence indicate the two major periods: an 8-year period during the 1950s and 1960s and a 2–3 year period in the last two decades. In the late 1970s, no remarkable period passed the significance test. The wavelet power spectrum of the simulated streamflows exhibits similar patterns to those of the observed flows, as shown in Figure 6. Two major period bands, an 8-year band from the year 1955 to 1964 and a 2–3-year band from the year 1995 to

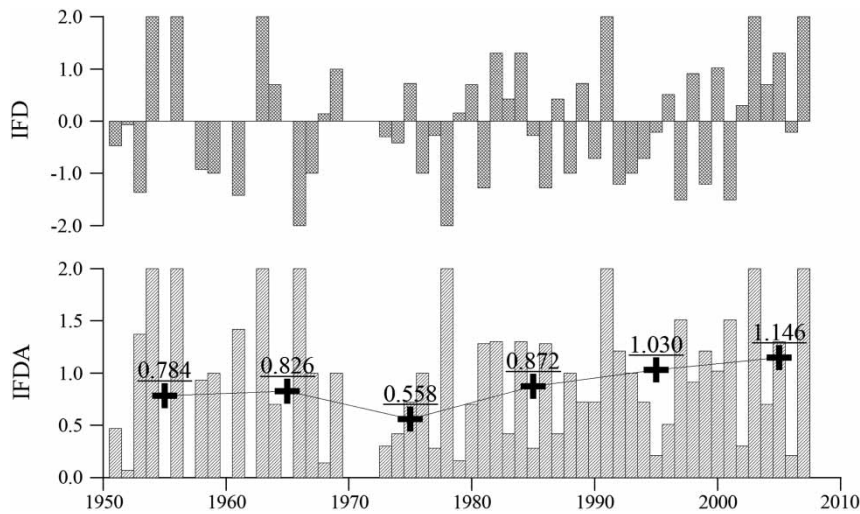


**Figure 4** | Composite indices of flood and drought from 1951 to 2007 in Huaihe River Basin.

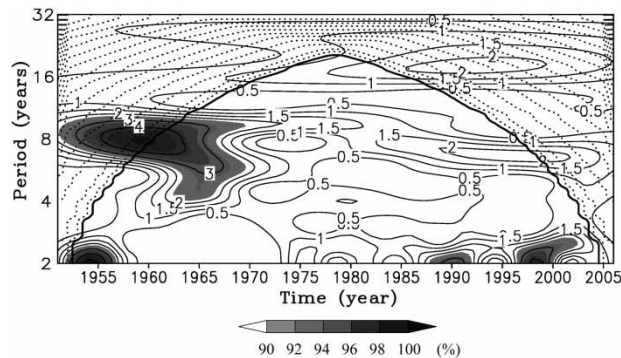


**Figure 5** | Period analysis of flood and drought based on observed streamflow.

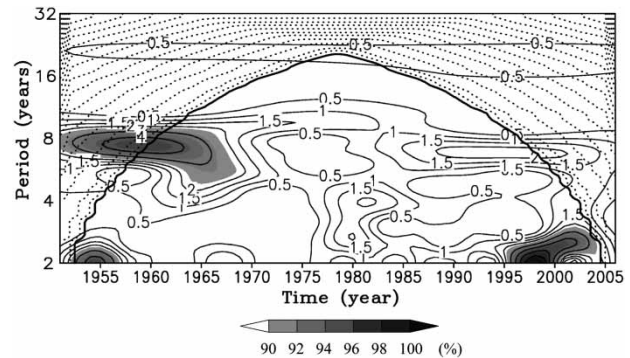


**Figure 6** | Period analysis of flood and drought based on simulated streamflow.

2004, passed the significance test. A period of approximately 4 years began at the start of the 1980s, although it did not reach the 90% confidence level.

Both of the two wavelet power spectra illustrate that flood and drought events occurred more frequently in 1990s and 2000s. Periods of flood and drought events were determined for different decades by the maximum of wavelet power spectrum. Typical periods, frequencies and corresponding years are summarized in Table 2 based on the observed and simulated streamflow series.

### Climate change and flood/drought events

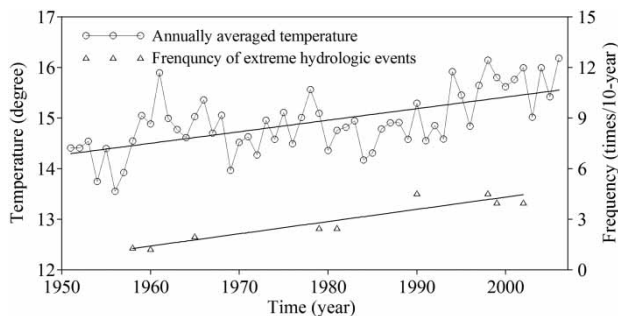
Temperature is a critical indicator of climate change. The IPCC report concluded that global surface temperature

increased by  $0.74 \pm 0.18$  °C in the last 100 years (1906–2005) due to greenhouse gas emissions by human activities (IPCC 2007). Average annual temperature from daily observed data fluctuated from 13.55 to 16.18 °C in the Huaihe River Basin from 1951 to 2006 (Figure 7). The basin has experienced a warming trend with a rate of 0.228 °C per decade, which is higher than the global average increase of 0.13 °C per decade (IPCC 2007). Average surface temperature has increased by approximately 1.28 °C since 1951. Most years of high temperature occurred in the late 1990s and 2000s; however, the highest temperature was recorded in 1961.

Observational evidence and climate model projections both support the theory that global warming leads to more extreme precipitation events (Allan & Soden 2008), which

**Table 2** | Peak position of wavelet spectra, period (year) and frequency of flood and drought (per decade) derived from observed and simulated streamflows for different decades

| Peak position | Observed streamflow |      |      |      |      | Simulated streamflow |      |      |      |
|---------------|---------------------|------|------|------|------|----------------------|------|------|------|
|               | 1960                | 1965 | 1979 | 1990 | 1999 | 1958                 | 1981 | 1998 | 2002 |
| Period        | 8                   | 5    | 4    | 2.2  | 2.5  | 7.5                  | 4    | 2.2  | 2.5  |
| Frequency     | 1.25                | 2.0  | 2.5  | 4.55 | 4    | 1.33                 | 2.5  | 4.55 | 4    |

**Figure 7** | Annual average temperature and frequency of flood and drought events in Huaihe River Basin from 1951 to 2006.

would result in more frequent and heavier floods and droughts. The frequency of flood and drought events is also plotted in Figure 7 (in open triangles) to compare with the warming trend in the Huaihe River Basin. A positive correlation with a coefficient of determination ( $R^2$ ) of 0.88 exists between the warming trend and the frequency of flood and drought events. The frequency of flood and drought events has tripled over the last six decades.

## CONCLUSIONS

The impact of climate change on water disasters in Huaihe River Basin was studied with the flood/drought grading method, the coupled land-surface hydrology model (LSX-HMS) and the Morlet wavelet transform approach.

The observed streamflow data cannot represent the natural response to local precipitation in recent dry years due to withdrawal of human activity; thus, a long-term continuous hydrologic simulation was conducted with the LSX-HMS model to rebuild the natural streamflows from 1951 to 2006. Composite indices of flood and drought (IFD) and absolute value of IFD (IFDA) were defined to quantify the flood/drought grades. The composite indices, combining the grades of flood and drought derived from

the time series of the observed rainfall, observed streamflow and simulated streamflow, assist in the avoidance of uncertainties on a single series. Temporal evolution of IFD and IFDA show that flood and drought events have occurred more frequently since 1980s.

Observed temperature indicates that Huaihe River Basin has experienced temperature rise with a trend of  $+0.228^\circ\text{C}$  per decade, especially in the last two decades. To examine possible relationships between climate change and water disasters, the frequency of flood and drought (quantified using the Morlet wavelet transform) was compared with the trend of average temperature. Flood and drought events are positively related to the climate warming with a coefficient of determination of 0.88.

Temperature is projected to increase with a higher rate according to the IPCC AR4 reports, resulting in heavier and more frequent floods and droughts in Huaihe River Basin and also in other regions of the world. The future water resources security for the basins involves huge challenges.

## ACKNOWLEDGEMENTS

This work is jointly supported by the National Basic Research Program of China (973 Program) (2010CB951101), the Programme of Introducing Talents of Discipline to Universities '111 Project' (B08048), the programme for Changjiang Scholars and Innovative Research Team in University (IRT0717) and the National Natural Science Foundation of China (NSFC) Projects (40830639 and 50679018).

## REFERENCES

- Allan, R. P. & Soden, B. J. 2008 *Atmospheric warming and the amplification of precipitation extremes*. *Science* **321**, 1481–1484.



- Bates, B. C., Kundzewicz, Z. W., Wu, S. & Palutikof, J. P. (eds.) 2008 *Climate Change and Water*. Technical Paper of the Intergovernmental Panel on Climate Change, IPCC Secretariat, Geneva, 210 pp.
- Burke, E. J., Brown, S. J. & Christidis, N. 2006 *Modelling the recent evolution of global drought and projections for the 21st century with the Hadley Centre climate model*. *J. Hydrometeorol.* **7**, 1113–1125.
- Chun, K. P., Wheeler, H. S. & Onof, C. J. 2009 *Streamflow estimation for six UK catchments under future climate scenarios*. *Hydrol. Res.* **40** (2–3), 96–112.
- Grinsted, A., Moore, J. C. & Jevrejeva, S. 2004 *Application of the cross wavelet transform and wavelet coherence to geophysical time series*. *Nonlinear Proc. Geoph.* **11**, 561–566.
- Hall, F. G., Meeson, B., Los, S., de Colstoun, E. & Landis, D. (eds.) 2005 ISLSCP Initiative II. NASA. DVD/CD-ROM. NASA.
- Houghton, J. T., Jenkins, G. J. & Ephraums, J. J. 1990 *IPCC First Assessment Report: Scientific Assessment of Climate Change-Report of Working Group I*. Intergovernmental Panel on Climate Change, Geneva.
- IPCC 2007 *Climate Change 2007: The Physical Science Basis. Contribution of Working Group I to the Fourth Assessment Report of the Intergovernmental Panel on Climate Change*. S. Solomon, D. Qin, M. Manning, Z. Chen, M. Marquis, K. B. Averyt, M. Tignor & H. L. Miller (eds.). Cambridge University Press, Cambridge, 996 pp.
- Jiang, T., Zhang, Q., Blender, R. & Fraedrich, K. 2005 *Yangtze Delta floods and droughts of the last millennium: abrupt changes and long term memory*. *Theor. Appl. Climatol.* **82** (3–4), 131–141.
- Kalney, E., Kanamitsu, M., Kistler, R., Collins, W., Deaven, D., Gandin, L., Iredell, M., Saha, S., White, G., Woollen, J., Zhu, Y., Leetmaa, A., Reynolds, R., Chelliah, M., Ebisuzaki, W., Higgins, W., Janowiak, J., Mo, K.C., Ropelewski, C., Wang, J., Jenne, R. & Joseph, D. 1996 *The NCEP/NCAR 40-year Reanalysis Project*. *Bull. Amer. Meteor. Soc.* **77**, 437–471.
- Kundzewicz, Z. 2004 *Detection of Change in World-Wide Hydrological Time Series of Maximum Annual Flow*. GRDC Report 32, 36 pp.
- Lehner, B., Döll, P., Alcamo, J., Henrichs, T. & Kaspar, F. 2006 *Estimating the impact of global change on flood and drought risks in Europe: a continental, integrated analysis*. *Climatic Change* **75** (3), 273–299.
- Meehl, G. A., Arblaster, J. M. & Tebaldi, C. 2005 *Understanding future patterns of precipitation intensity in climate model simulations*. *Geophys. Res. Lett.* **32**, L18719.
- Meteorological Institute of the Chinese Meteorological Bureau (MICMB), (eds.) 1981 *Atlas of the Flood/Dryness in China for the Last 500-Year Period*. Cartological Press, Beijing, China (in Chinese).
- Milly, P. C. D., Wetherald, R. T., Dunne, K. A. & Delworth, T. L. 2002 *Increasing risk of great floods in a changing climate*. *Nature* **415**, 514–517.
- Nakken, M. 1999 *Wavelet analysis of rainfall-runoff variability isolating climatic from anthropogenic patterns*. *Environ. Modell. Softw.* **14**, 283–295.
- Pollard, D. & Thompson, S. L. 1995 *Use of a land-surface-transfer scheme (LSX) in a global climate model: the response to doubling stomatal resistance*. *Glob. Planet. Change* **10**, 129–161.
- Qian, M. 2008 *Flood control and Huaihe River Flood in 2007*. *Water Resour. Hydropower Eng.* **39** (1), 12–15 (in Chinese).
- Sheffield, C. & Wood, E. F. 2008 *Global trends and variability in soil moisture and drought characteristics 1950–2000, from observation-driven simulations of the terrestrial hydrologic cycle*. *J. Clim.* **21**, 432–458.
- Torrence, C. & Compo, G. P. 1998 *A practical guide to wavelet analysis*. *B. Am. Meteorol. Soc.* **79**, 61–78.
- Vejjalainen, N. & Vehviläinen, B. 2008 *The effect of climate change on design floods of high hazard dams in Finland*. *Hydrol. Research* **39**, 465–477.
- Waters, D., Watt, W. E., Marsalek, J. & Anderson, B. C. 2003 *Adaptation of a storm drainage system to accommodate increased rainfall resulting from climate change*. *J. Environ. Plan. Manage.* **46**, 755–770.
- Werrity, A., Black, A., Duck, R., Finlinson, B., Thurston, N., Shackley, S. & Crichton, D. 2002 *Climate Change: Flooding Occurrences Review*. Scottish Executive Central Research Unit, Edinburgh, 94 pp.
- Wetherald, R. T. & Manabe, S. 2002 *Simulation of hydrologic changes associated with global warming*. *J. Geophys. Res.* **107** (D19), 4379.
- Yang, C., Lin, Z., Yu, Z., Hao, Z. & Liu, S. 2010 *Analysis and simulation of human activity impact on streamflow in the Huaihe River Basin with a large-scale hydrologic model*. *J. Hydrometeorol.* **11**, 810–821.
- Yu, Z. 2000 *Assessing the response of subgrid hydrologic processes to atmospheric forcing with a hydrologic model system*. *Global Planet. Change* **25**, 1–17.
- Yu, Z., Lakhtakia, M. N. & Barron, E. J. 1999 *Modeling the river basin response to single-storm events simulated by a mesoscale meteorological model at various resolutions*. *J. Geophys. Res.* **104**, 19675–19690.
- Yu, Z., Pollard, D. & Cheng, L. 2006 *On continental-scale hydrologic simulations with a coupled hydrologic model*. *J. Hydrol.* **331**, 110–124.
- Zhang, Q., Chen, J. & Becher, S. 2007 *Flood/drought change of last millennium in the Yangtze Delta and its possible connections with Tibetan climatic changes*. *Global Planet. Change* **57**, 213–221.
- Zhou, Y., Ma, Z. & Wang, L. 2002 *Chaotic dynamics of the flood series in the Huaihe River Basin for the last 500 years*. *J. Hydrol.* **258**, 100–110.